OST 1

DOE/ER/45261--1

DE89 012577

DOE/ER/45261--1

STRUCTURAL DISORDER AND TRANSPORT IN TERNARY OXIDES WITH THE PYROCHLORE STRUCTURE

submitted by
H.L. Tuller, Principal Investigator
Crystal Physics & Optical Electronics Laboratory
Department of Materials Science & Engineering
Massachusetts Institute of Technology
Cambridge, MA 02139

to

Basic Energy Sciences
Department of Energy
Attn: Dr. Jules Routbort

Harry L. Tuller, Professor
Ceramics and Electronic Materials

Merton C. Flemings, Head
Dept. of Materials Science & Engineering

George H. Dummer, Director
Office of Sponsored Research

DISTRIBUTION OF THIS DOCUMENT IS UNLIMITED

(Proposed Research part of report has been removed)

SUMMARY OF PREVIOUS WORK

Our first two years of work on pyrochlore compounds under this program have been very productive. We have been able to tie changes in the electrical conductivity to variations of the structural disorder in the $Gd_2(Zr_xTi_{1-x})_2O_7$ pyrochlore solid solution. This has enabled us to improve our scientific understanding of the source of fast ion conduction in these systems. It has also led to insights into methods for tailoring the electrical properties in order to achieve a wide range of useful characteristics. We now have the ability to make intrinsic solid electrolytes, mixed conductors, semiconductors,

and insulators from $Gd_2(Zr_xTi_{1-x})_2O_7$ by manipulating the composition and dopant content. In the following, we discuss some of these observations.

Defect Model

As expected, GZT is a mixed ionic-electronic conductor with the electronic component increasing with increasing fraction of multi-valent Ti cation on the B-site. A defect chemical model was developed which enabled us to:

(a) deconvolute the n and p type semiconductive components and ionic component from the total conductivity,

(b) determine the nature of the mobile oxygen species, and

(c) derive a number of key thermodynamic parameters including those related to intrinsic disorder.

The key defect relations found adequate to describe both the GZT and YZT systems under nearly all experimental conditions are summarized in Table 1 (see Eqs. 1-4). The choice of anion frenkel disorder is consistent with the known tendency of pyrochlores to disorder into the fluorite structure.

For intermediate Po_2's, and low doping levels, the electroneutrality relation simplifies to

$$[V_o^{\cdot\cdot}] = [O_i''] = K_F^{1/2} \qquad (5)$$

where K_F is the frenkel equilibrium constant (See Eq. 1). These conditions, as we demonstrate below, are appropriate for the

majority of our experimental results. Substituting Eq. 5 into Eq.3, and solving for the electron density n, one finds

$$n = \left(\frac{K_r}{K_F^{1/2}}\right)^{1/2} \quad Po_2^{-1/4} \tag{6}$$

Combining Eq. 6 with Eq. 2, one obtains a similar expression for the hole density p

$$p = K_i\left(\frac{K_F}{K_r}^{1/2}\right)^{1/2} \quad Po_2^{+1/4} \tag{7}$$

Thus, one can distinguish the n, p, and ionic components of the total conductivity by their Po_2 dependencies and extract key enthalpies from their temperature dependence measured at constant Po_2.

As an example, we show the bulk conductivities measured for $Gd_2(Zr_{0.3}Ti_{0.69}Ta_{0.01})_2O_7$ as a function of Po_2 for a series of isotherms ranging from 800°C to 1100°C at 100°C intervals in Fig. (4). The data can readily be fit to an expression of the form

$$\log \sigma = \log [\ A + BPo_2^{-1/4} + CPo_2^{+1/4}] \tag{8}$$

where A,B, and C are independent of Po_2 but are functions of temperature. A represents the ionic conductivity, $BPo_2^{-1/4}$ the n-type conductivity and $CPo_2^{+1/4}$ the p-type conductivity (see Eqs. 5-7) Fig. (4) shows the results of fitting Eq. 8 (curved lines) to the experimental data (filled circles) and the

individual conductivity components (straight lines). One readily observes that for this donor doped, Ti-rich solid solution, the conductivity is predominantly n-type at low Po_2 and mixed with significant ionic and hole contributions at high Po_2.

As the Zr fraction is increased, the ionic conductivity systematically increases at the expense of the electronic component as illustrated in Fig. (5) for $Gd_2(Zr_{0.6}Ti_{0.4})_2O_7$. Here, the Po_2-independent component controls under all conditions but for the highest temperatures and lowest Po_2's. For x = 1 (not shown), no Po_2-dependent conductivity is observed under similar experimental conditions.

From an analysis of the electronic components of the conductivity, utilizing our defect chemical model, we have determined both the enthalpy of reduction and the bandgap energy as a function of x in GZT. These are listed in Table 2. The band gap energy of approximately 4eV is in good agreement with optical absorption measurements we have performed on $Gd_2Ti_2O_7$ from which we extract an optical band gap of about 3.8eV.

The reduction enthalpy E_r increases from 4.8eV at x = 0 to over 6eV at higher x. The increase is expected since the multivalent Ti ion, which provides a lower energy path for reduction, is being diluted. At larger x, the determination of E_r becomes less reliable given the small electronic contribution which becomes successively more difficult to deconvolute from the total conductivity. A more refined analysis which takes into

account simultaneous contributions from both intrinsic and extrinsic sources is presently being prepared for publication[11] (see following section).

Ionic Conductivity

The ionic conductivity, which is plotted as a function of x in Fig. (6). is observed to increase nearly 100,000-fold between x = 0.15 and 0.8 with the steepest increase occuring between x = 0.15 and 0.3. The increase in the ionic conductivity with x is consistent with our initial expectations, i.e., that as we approach the pyrochlore-fluorite phase boundary by decreasing the R_A/R_B ratio, the material would become systematically more disordered. Several doping experiments were used to (a) confirm that intrinsic anionic disorder was responsible for the high ionic conductivities at larger values of x, (b) establish that the source of the large increase in ionic conductivity with x in Fig. (6) was due primarily to disordering rather than an increase in ionic mobility, and (c) determine the magnitude of the intrinsic disorder.

In Fig. (7), we show the temperature dependence of the ionic conductivity of the zirconate end member both undoped and acceptor doped with 1 mol% Ca. The two results are essentially identical demonstrating that the high ionic conductivity is due to intrinsic disorder rather than doping, as in stabilized zirconia, for example. Thus, GZT (x=1) is an intrinsic fast ion conductor such as Bi_2O_3, rather than an extrinsic fast ion conductor such as stabilized ZrO_2.

With the ionic conductivity of GZT (x = 0.3) being a 100-fold lower than the GZT (x= 1.0) end member, we expected, and found, both intrinsic and extrinsic contributions to the conductivity of the x = 0.3 material upon doping as illustrated in Fig. (8). Fitting these data to an extension of our defect model,[12] which includes contributions from both intrinsic and impurity induced ionic defects, enabled us to extract both the oxygen vacancy mobility and the effective frenkel equilibrium constant which are seen plotted in Fig. (9) as a function of reciprocal temperature. Note the anomalously high values of both μ_{v_o} and K_F for this material. Further, note that the ionic conductivity increases with acceptor doping and decreases with donor doping. This clearly demonstrates that ionic conduction in these materials is dominated by oxygen vacancy rather than oxygen interstitial diffusion.

In Figs. (10) and (11), we present the pre-exponential constant and the activation energy for ionic conduction, respectively, as a function of x, where

$$\sigma T = \sigma_o \exp(-E/kT) \qquad (9)$$

The near linear increase of log σ_o, coupled with the near independence of E (for undoped specimens) with x, strongly suggests that the sharp increase in ionic conductivity is due to a corresponding increase in charge carrier concentration rather than a change in mobility with x. Since we have shown (a) that intrinsic disorder dominates the ionic conductivity in Fig. (6)

from at least x = 0.3 to 1.0, and (b) that the conductivity increase is predominantly carrier controlled, we can therefore conclude that the anion sublattice in the GZT disorders monotonically with increasing x, as initially assumed. In the following, we discuss the structural disorder more explicitly.

STRUCTURAL DISORDER

Cation Disorder

In the ideal pyrochlore structure, the A and B cations occupy distinct sites but in the defect fluorite structure they are distributed at random. Defect pyrochlores are intermediate between these two extremes having a few A cations on the B sites and a few B cations on the A sites. This disorder can be quantified with the cation order parameter (Φ_c), defined as:

$$\Phi_c = \frac{A_A - A_A(F)}{A_A(P) - A_A(F)} \qquad (10)$$

where A_A is the actual A ion occupation of the A site and $A_A(F)$ and $A_A(P)$ are the A ion occupation of the A site assuming ideal defect fluorite and ideal pyrochlore structures respectively. Since, ideal defect fluorite is perfectly random and ideal pyrochlore is perfectly ordered:

$$\Phi_c = \frac{A_A - \frac{1}{2}}{1 - \frac{1}{2}} = 2A_A - 1 \qquad (11)$$

The cation order parameter may be estimated from the intensity of selected x-ray diffraction peaks. We have[7] used the ratio of the intensity of the [331] and [400] peaks to calculate the cation order parameter as a function of composition throughout the $Gd_2(Zr_xTi_{1-x})_2O_7$ solid solution. The cation order parameter decreases monotonically from 1.0 to 0.65 as x varies from 0 to 1. The cation "disorder" parameter $(1-\phi_c)$, shown plotted in Fig. (6), increases with x as does the ionic conductivity. These data must be treated cautiously since the cation order parameter can not be rigorously determined from only two diffraction peaks. Nevertheless, the trend in the data is firmly established.

Anion Disorder

A similar analysis[7,13] for the anion sublattice leads to the following equation for the anion order parameter:

$$\phi_A = 8(O_{48f} - 7/8) \qquad (12)$$

where the 48f oxygen sites represent the most likely location for mobile oxygen vacancies.

The oxygen vacancy concentration can be estimated from the pre-exponential constant for ionic conductivity of the $Gd_2(Zr_xTi_{1-x})_2O_7$ system using an atomistic model for the ionic conductivity.

For unassociated carriers, it can be shown that

$$\sigma_o = \frac{4\alpha e^2 a^2 v_o N_o [V_o^{\cdot\cdot}] \exp(S_M/k)}{k} \qquad (13)$$

where σ_o is the pre-exponential constant for ionic conductivity, α is a geometrical factor, e is the elementary charge, a_o is the carrier jump distance, v_o is the jump attempt frequency, N_o is the number of oxygen 48f sites per unit volume, $V_o^{\cdot\cdot}$ is the fractional oxygen 48f site vacancy concentration, S_M is the migration entropy and k is Boltzmann's constant. The order parameter (Φ_A) can then be calculated from Eq. (12) where the fractional 48f site occupancy (O_{48f}) is equal to one minus the fractional vacancy concentration $[V_o^{\cdot\cdot}]$.

The anion order parameter follows the same trend as the cation order parameter. Thus, as the Zr content increases both the cation and anion sublattices become disordered leading to a sharp increase in ionic conductivity as shown in Fig. (6). The substantial disorder present in $Gd_2(Zr_xTi_{1-x})_2O_7$ with $x \geq 0.4$ and the low activation energy of conduction makes these compositions qualify as intrinsic fast ion conductors.

Recent work has concentrated on characterizing the $Y_2(Zr_xTi_{1-x})_2O_7$ (YZT) system by systematic and exhaustive electrical measurements. This system, in contrast to GZT, can be studied by neutron diffraction techniques (Gd is a strong neutron absorber). Since disorder on the oxygen sublattice can be most

effectively examined by neutrons, this will allow for a more effective correlation to be made between oxygen ion transport and structure.

A comparison between the properties of the GZT and YZT system becomes of interest due to their different lattice parameters (See Fig. 2) and different cation order parameters for equivalent values of x. A similar large jump in ionic conduction occurs at intermediate x in YZT as it does in GZT but, as Fig. (11) shows, the ionic migration energy is significantly larger in the YZT system. Understanding the reason for this large change will be a major objective of our future work.

The final portion of our proposed research involves a collaboration with Professor C.R.A. Catlow at the University of Keene in the United Kingdom. Computer modeling methods are now used extensively in solid state chemistry with fast ion conductors being a particularly active subfield in this regard. The key modeling methods used[16] have three main aims.

(1) to predict the structures and properties of materials,

(2) to describe the behavior of defects, and

(3) to elucidate the detailed mechanisms of atomic migration.

Most calculations in the first two categories use static simulations while the third requires dynamical methods. Professor Catlow has had excellent success in recent years in applying both approaches to a number of oxide and fluoride systems[17,18]. In particular, we will be looking to clarify the following points: (a) establishing the most energetically favorable sites for oxygen vacancies thereby suggesting the most favorable pathways for oxygen diffusion, (b) calculating structural disorder as a function of composition and cation radius ratio, and (3) predicting candidate compositions with attractive properties.

REFERENCES

1. W.W. Barker, J. Graham, O. Knop, and F. Brisse, Crystal Chemistry of Oxide Pyrochlores, " The Chemistry of Extended Defects in Non-Metallic Solids," E.L. Eyring and M. O'Keefe, North Holland Publishing Co., (1970).

2. Ronald A. McCauley, "Structural Characteristics of Pyrochlore Formation," J. Appl. Phys. 51(1) p. 290 (1980).

3. E.M. Logothetis, "ZrO_2 Oxygen Sensors in Automotive Application," Advances in Ceramics, Vol. 3, ed. A.H. Heuer and L.W. Hobbs, 1981.

4. H.L. Tuller, "Mixed Conduction in Nonstoichiometric Oxides," in Non-Stoichiometric Oxides, ed. O.T. Sorensen, Academic Press, NY (1981), pp. 271-335.

5. H.S. Horowitz, M.M. Longo, and H.H. Horowitz, "Oxygen Electrocatalysis on Some Oxide Pyrochlores," J. Electrochem. Soc. 130 1851-59 (1983).

6. R.W. Vest, "Conduction Mechanisms in Thick Film Microcircuits," Final Rept., ARPA No. 1642, 1975 (NTIS No. N76-13346).

7. H.L. Tuller and P.K. Moon, "Fast Ion Conductors-Future Trends, Mat. Sc. Eng. B., in print.

8. T. van Dijk, K.J. DeVries, and A.J. Burggraaf, "Electrical Conductivity of Fluorite and Pyrochlore in $Ln_xZr_{1-x}O_{2-x/2}$ (Ln = Gd, Nd) Solid Solutions," Phys. Stat. Sol. (a) 58,115 (1980).

9. R.D. Shannon and C.T. Prewitt, "Effective Ionic Radii in Oxides and Fluorides," Acta Cryst. B25 925 (1969).

10. W.E. Klee and G. Weitz, "Infrared Spectra of Ordered and Disordered Pyrochlore-type compounds in the Series $RE_2Ti_2O_7$, $RE_2Zr_2O_7$ and $RE_2Hf_2O_7$," J. Inorg. Nucl. Chem. 31 2367 (1969).

11. P.K. Moon, M.A. Spears, and H.L. Tuller, "The Defect Chemistry of Pyrochlore Solid Solutions of the Type $R_2(Ti_{1-x}Zr_x)_2O_7$ with R=Gd,Y," Materials Res. Soc. Proc., December 1988, Boston, MA in preparation.

12. P.K. Moon and H.L. Tuller, "Ionic Conduction in the $Gd_2Ti_2O_7$-$Gd_2Zr_2O_7$ System," in Proc. 6th Intl. Conf. on Solid State Ionics, September 6-11, 1987, Garmisch, Germany, Solid State Ionics, in press.

13. P.K. Moon, "Electrical Conductivity and Structural Disorder in $Gd_2Ti_2O_7$-$Gd_2Zr_2O_7$ and $Y_2Ti_2O_7$-$Y_2Zr_2O_7$ Solid Solutions," Ph.D. Thesis, MIT, Cambridge, MA, 1988.

14. H.L. Tuller, J.A. Kilner, A.E. McHale, and B.C.H. Steele, "Oxygen Diffusion in Oxygen Excess CeO_2-UO_2 Solid Solutions," in Reactivity of Solids, eds. P. Barrett and L.C. Dufour, Elsevier, Amsterdam (1985) pp. 315-19.

15. M. Oueslati, M. Balkanski, P.KL. Moon, and H.L. Tuller, "Raman Spectroscopy and Structural Disorder in $Gd_2(Zr_xTi_{1-x})_2O_7$," Materials Research Society Proc., December 1988, Boston, MA, in preparation.

16. C.R.A. Catlow, "Static Lattice Simulation of Structure and Transport in Superionic Conductors," Solid State Ionics 8 pp. 89-107 (1983).

17. M.P. Van Dijk, A.J. Burggraaf, A.N. Cormack, and C.R.A. Catlow," Defect Structure and Migration Mechanisms in Oxide Pyrochlores," Solid State Ionics, 17 pp. 159-67 (1985).

18. C.R.A. Catlow, "Transport in Doped Fluorite Oxides," Solid State Ionics, 12 pp. 67-73 (1984).

19. M.P. Pechini, "Method of Preparing Lead and Alkaline Earth Titanates and Niobates and Coating Method Using the Same to Form a Capacitor," U.S. Patent 3,330,697 (1967).

20. N.G. Eror and D.M. Smyth, "Oxygen Stoichiometry of Donor-Doped $BaTiO_3$ and TiO_2," in The Chemistry of Extended Defects in Non-Metallic Solids, ed. L. Eyring and M. O'Leefe, North Holland (1970).

Table I: Defect Relations

Intrinsic Ionic Disorder:

$$O_o^x \rightarrow V_o^{\cdot\cdot} + O_i'' \qquad (1)$$

Intrinsic Electronic Disorder:

$$nil \rightarrow e' + h^{\cdot} \qquad (2)$$

$$n\,p = K_i = K_{i\,o}\ \exp(-E_g/kT)$$

Redox Equilibria:

$$O_o^x \rightarrow V_o^{\cdot\cdot} + 1/2O_2 + 2e' \qquad (3)$$

$$[V_o^{\cdot\cdot}]n^2 Po_2^{1/2} = K_r = K_{r\,o}\exp(-E_r/kT)$$

Electroneutrality:

$$2[V_o^{\cdot\cdot}] + p + [Ta_B^{\cdot}] = 2[O_i''] + n + [Ca_A'] \qquad (4)$$

([Ca_A'] and [$Ta_B^{\cdot}$] correspond to acceptor and donor dopants respectively)

Table 2: The enthalpy of reduction and the thermal bandgap for $Gd_2(Zr_xTi_{1-x})_2O_7$

Composition*	E_B (eV)	E_C (eV)	E_g (eV)	E_F (eV)
GZTO	2.4	-	-	4.8
GZTO + 1.0%Ca	2.4	-	-	4.8
GZT15	2.6	-	-	5.2
GZT30	3.2	0.9	4.1	6.4
GZT30 + 0.5%Ca	3.0	1.3	4.3	6.0
GZT30 + 1.0%Ca	3.4	1.2	4.6	6.8
GZT30 + 1.0Ta	2.9	1.0	3.9	5.8
GZT40	3.0	1.0	4.0	6.0
GZT50	3.6	0.8	4.4	7.2
GZT60	3.1	-	-	6.2

*Compositions are designated with the letters GZT followed by the percent Zr content, for example $Gd_2(Zr_{0.3}Ti_{0.7})_2O_7$ is designated as GST30.

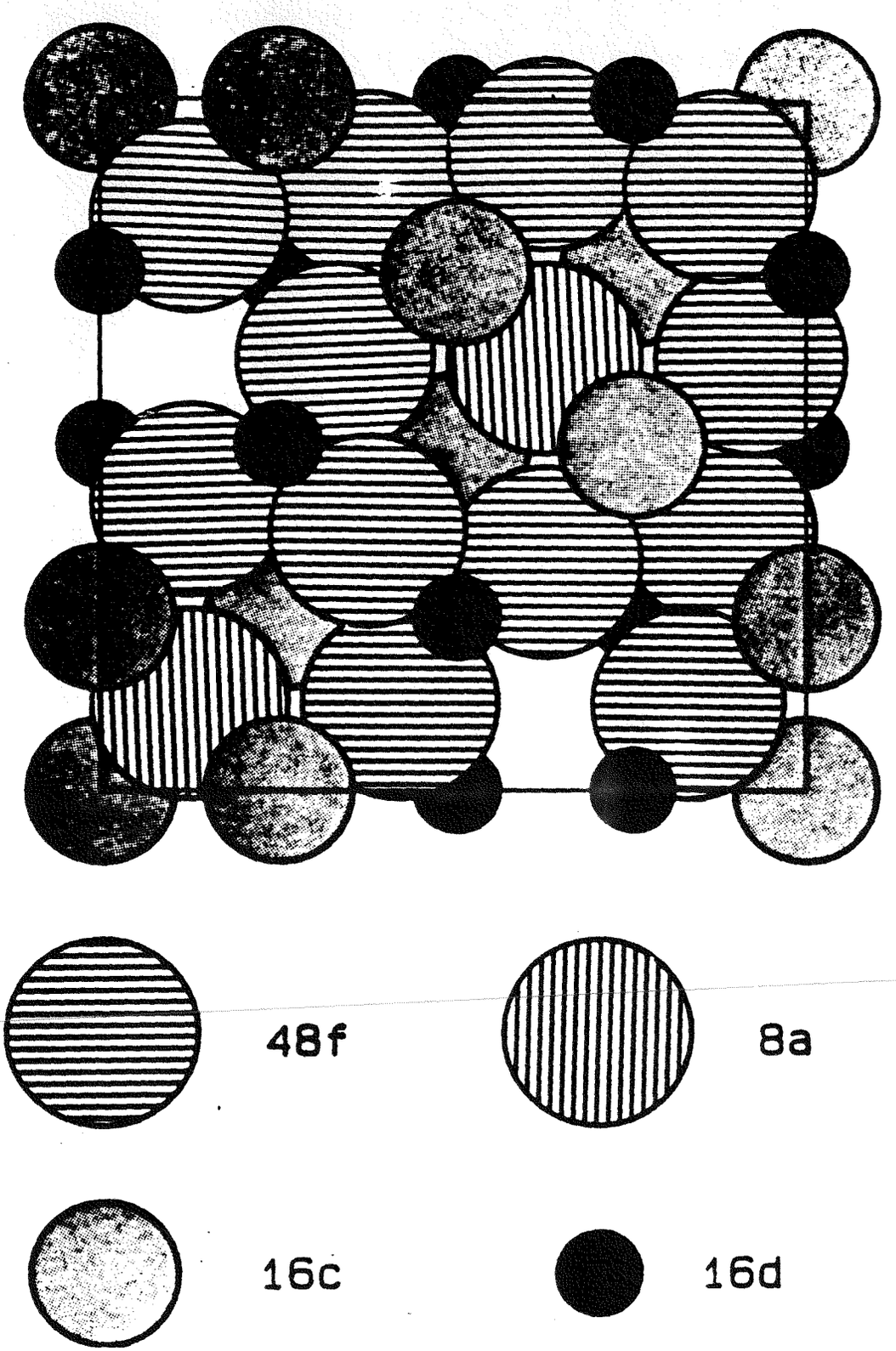

Fig. 1: (100) projection of a portion of one unit cell of the pyrochlore structure.

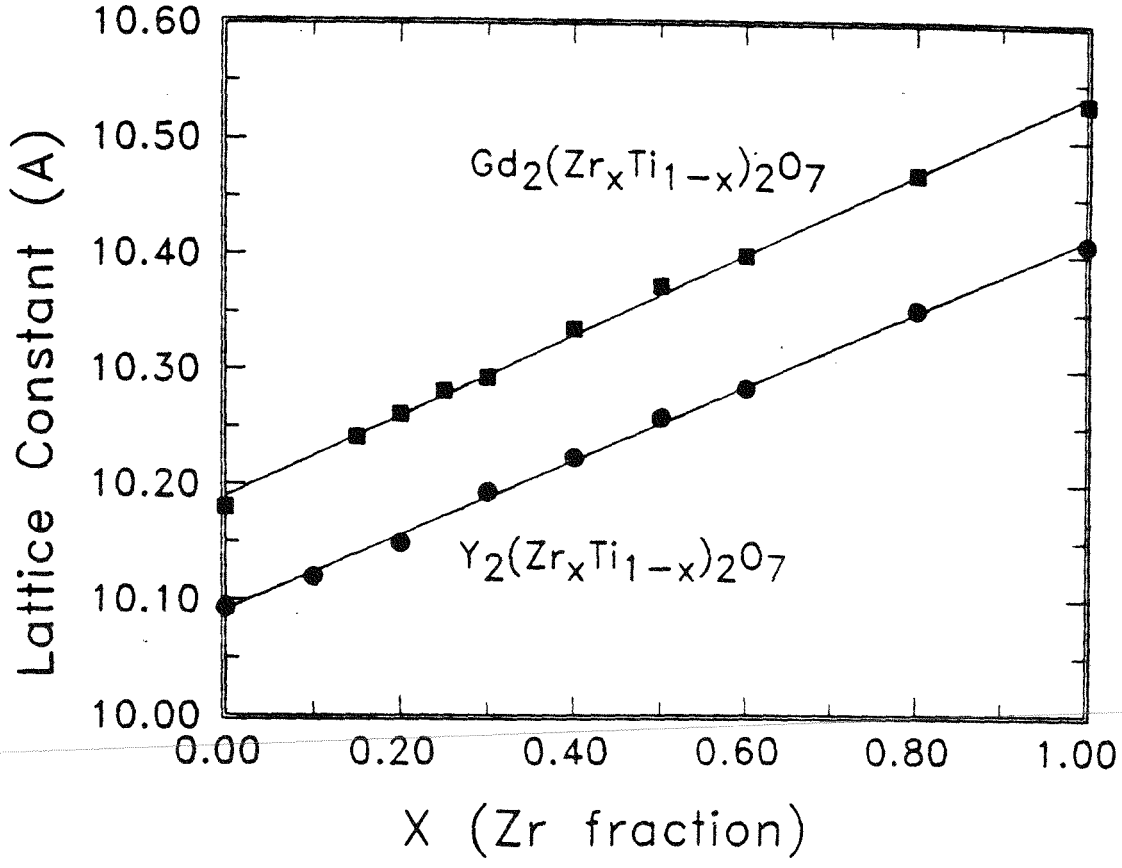

Fig. 2: Lattice constants of GZT and YZT as a function of Zr fraction.

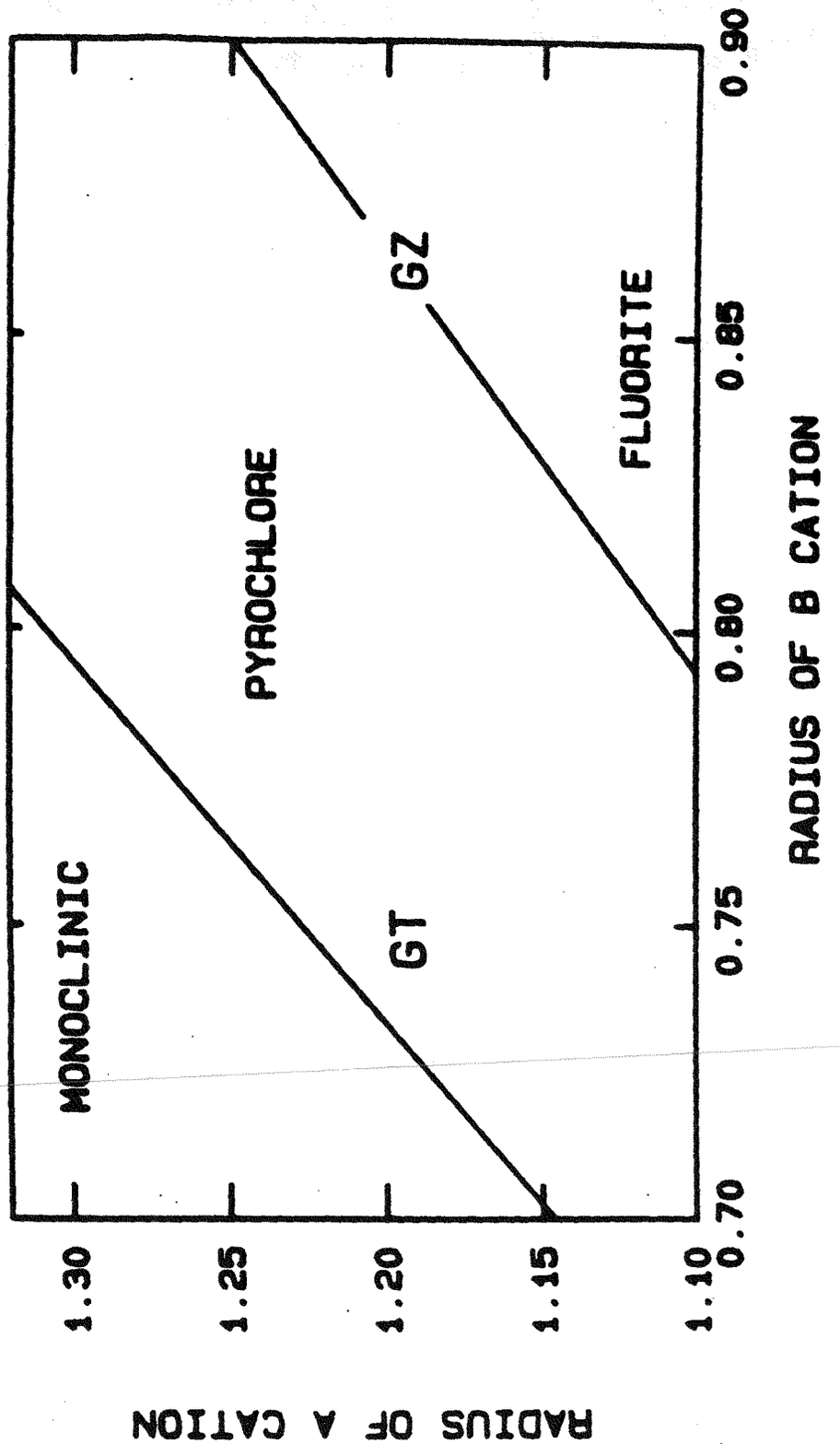

Fig. 3: The pyrochlore stability field as a function of the cation radii. GT and GZ represent the titanate and zirconate end members in the GZT system.

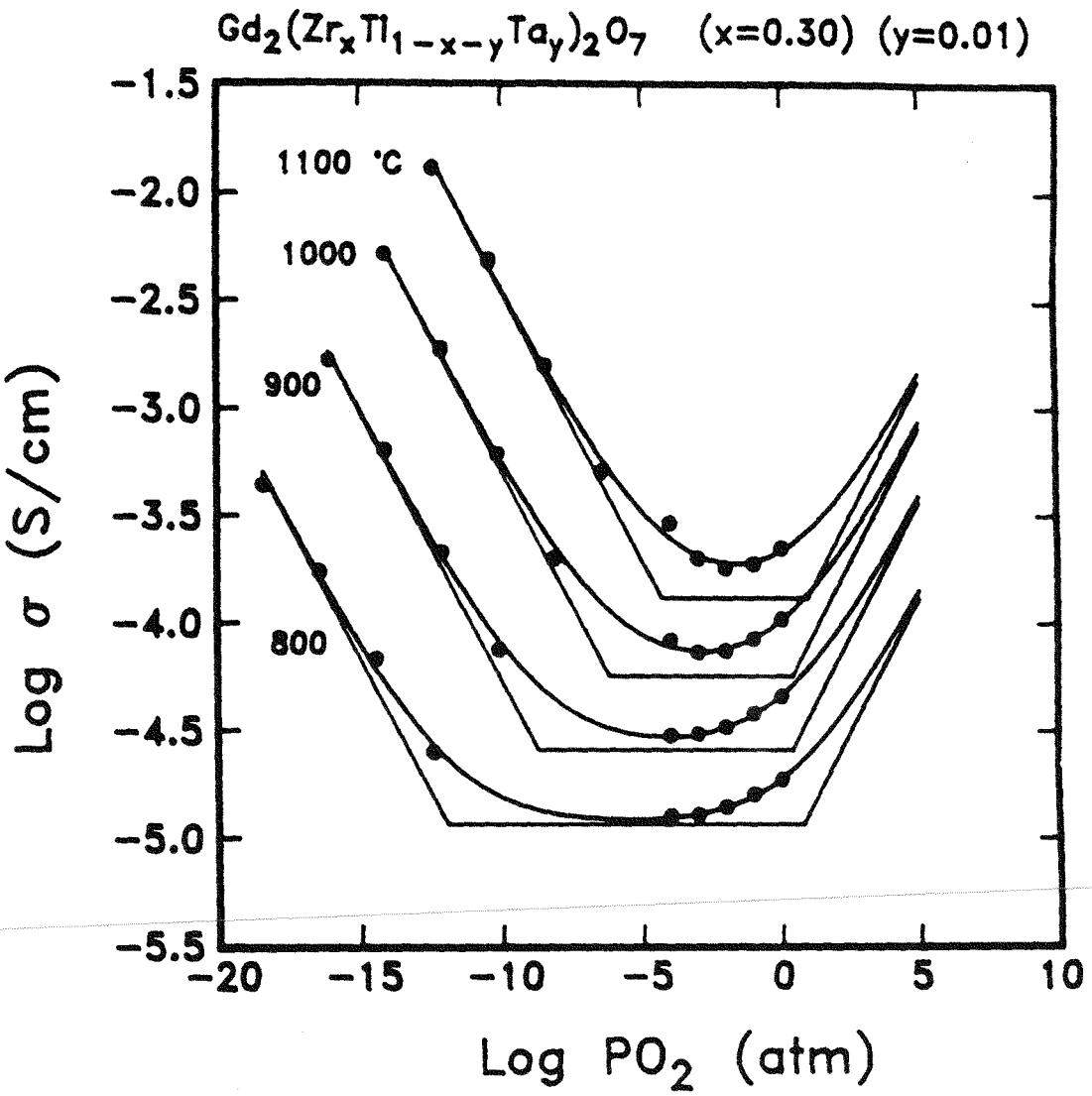

Fig. 4: Log conductivity versus log oxygen partial pressure for $Gd_2(Zr_{0.3}Ti_{0.69}Ta_{0.01})_2O_{7+\delta}$ showing the least squares fit of Eq. 8 to the experimental data.

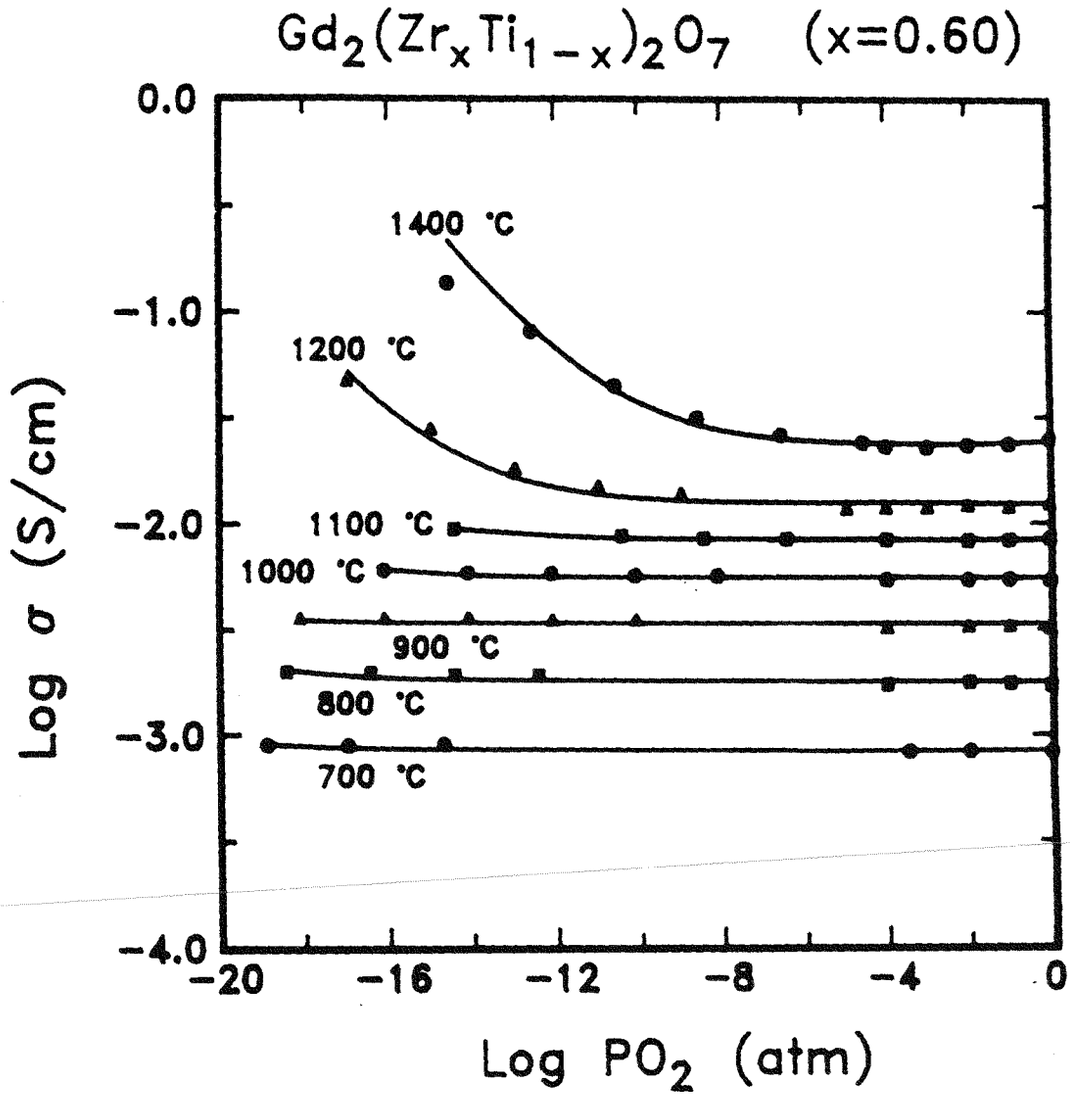

Fig. 5: The log conductivity as a function of log oxygen partial pressure for $Gd_2(Zr_{0.6}Ti_{0.4})_2O_7$.

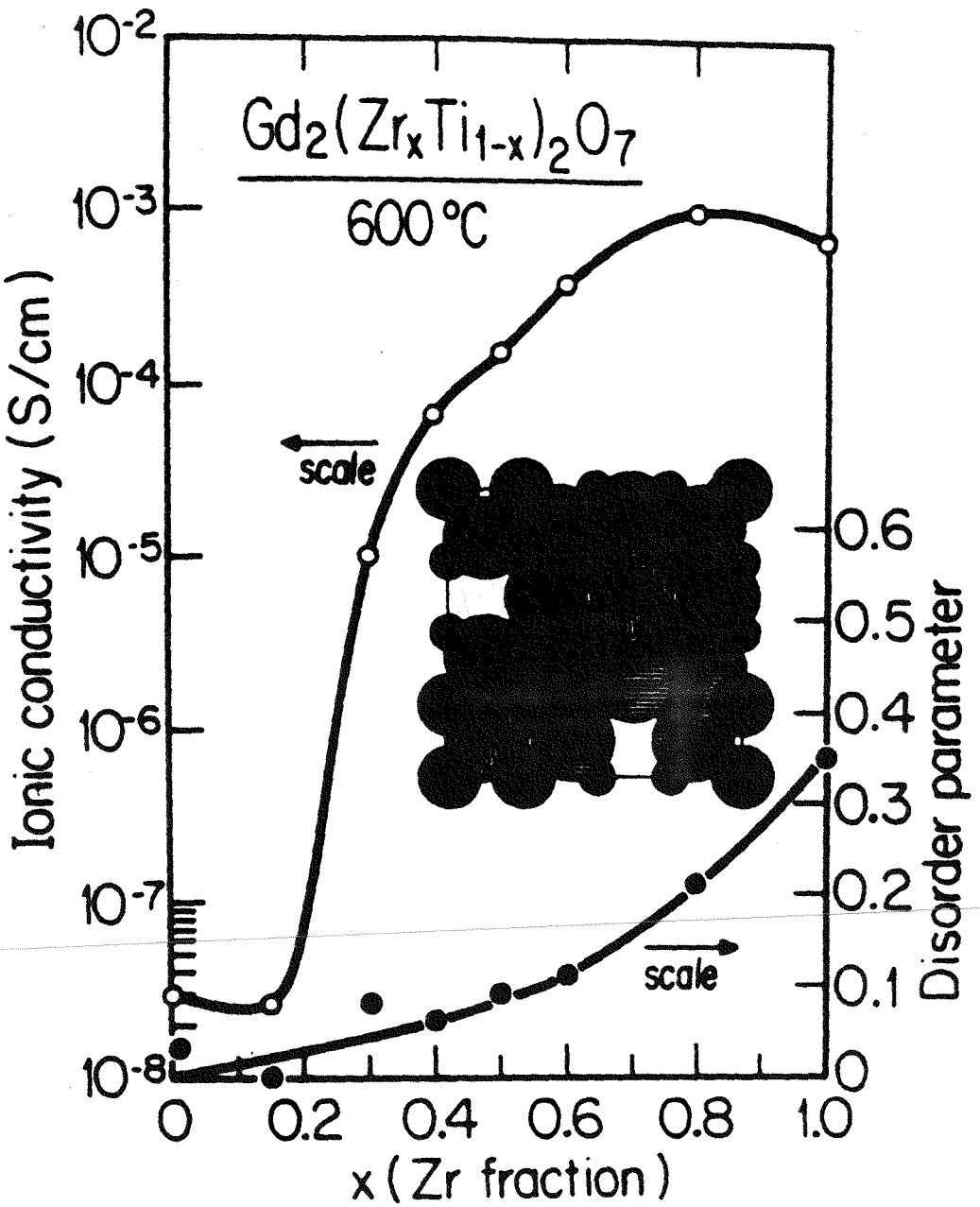

Fig. 6: Ionic conductivity measured at 600°C and the cation disorder parameter as a function of Zr fraction in GZT.

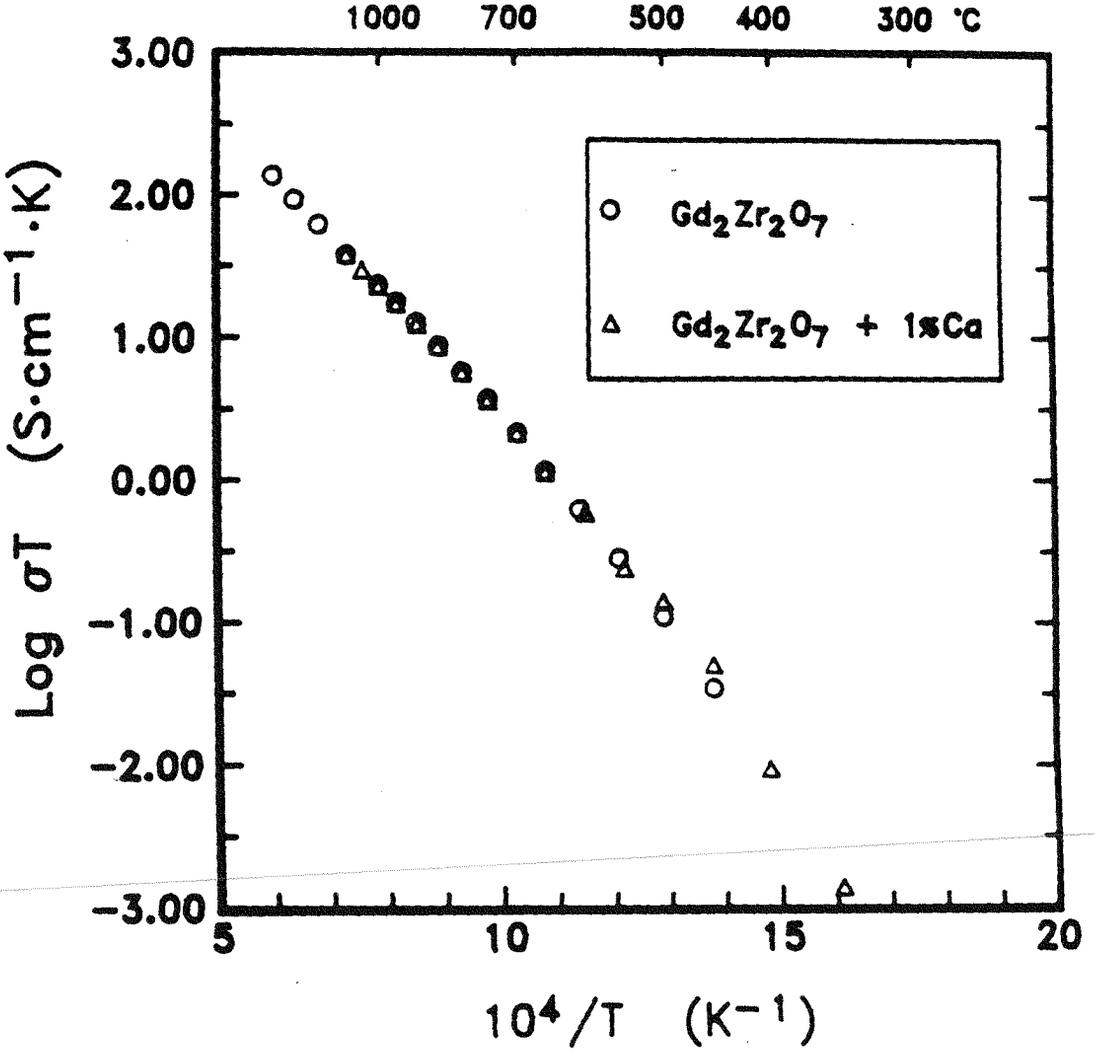

Fig. 7: An Arrhenius plot of the conductivity of $Gd_2Zr_2O_7$ and $(Gd_{0.99}Ca_{0.01})_2Zr_2O_{7-\delta}$.

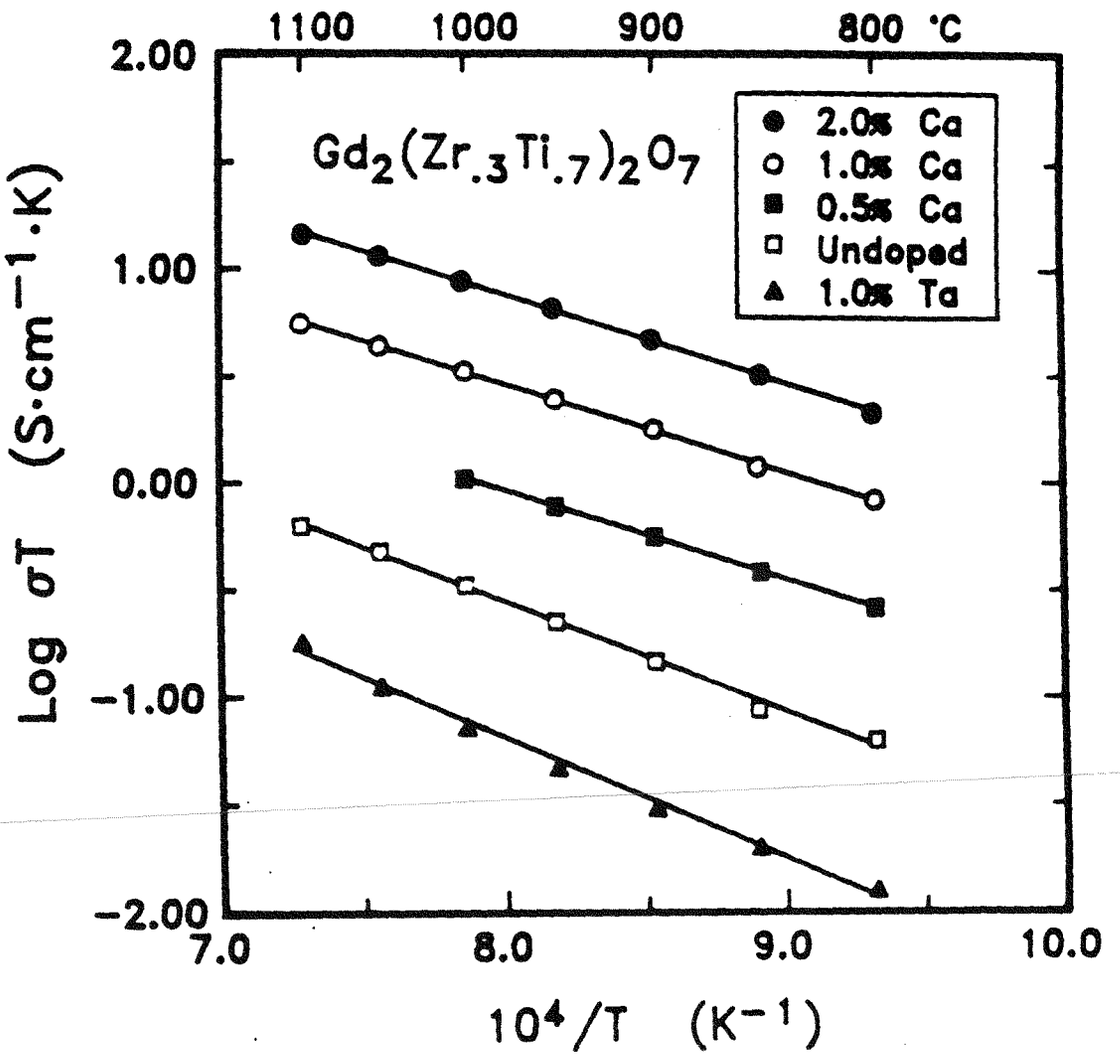

Fig. 8: Arrenhius plots of the ionic conductivity for doped and nominally pure $Gd_2(Zr_{0.3}Ti_{0.7})_2O_7$.

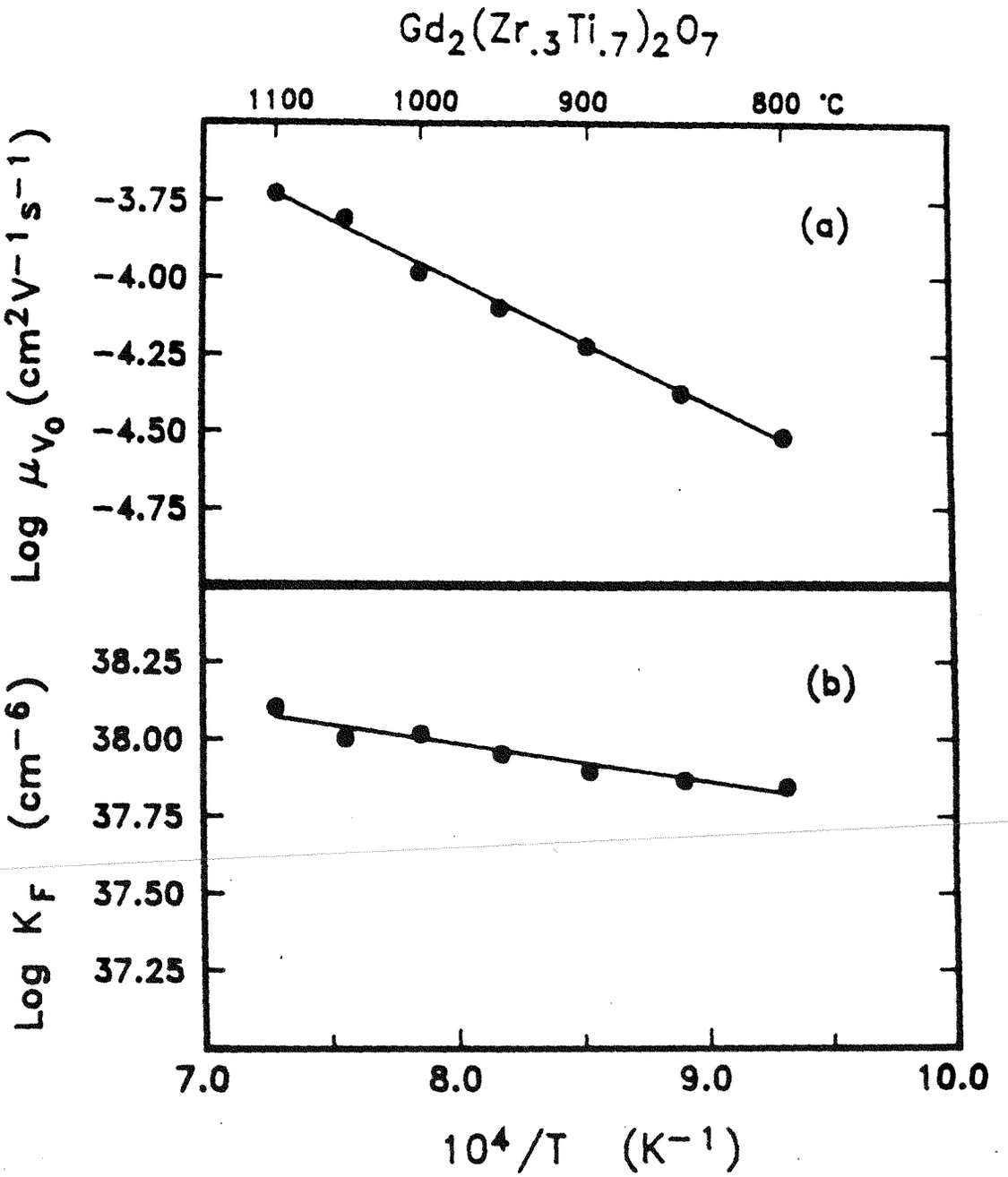

Fig. 9: Arrenhius plots of (a) the oxygen vacancy mobility and (b) the anion Frenkel constant for $Gd_2(Zr_{0.3}Ti_{0.7})_2O_7$.

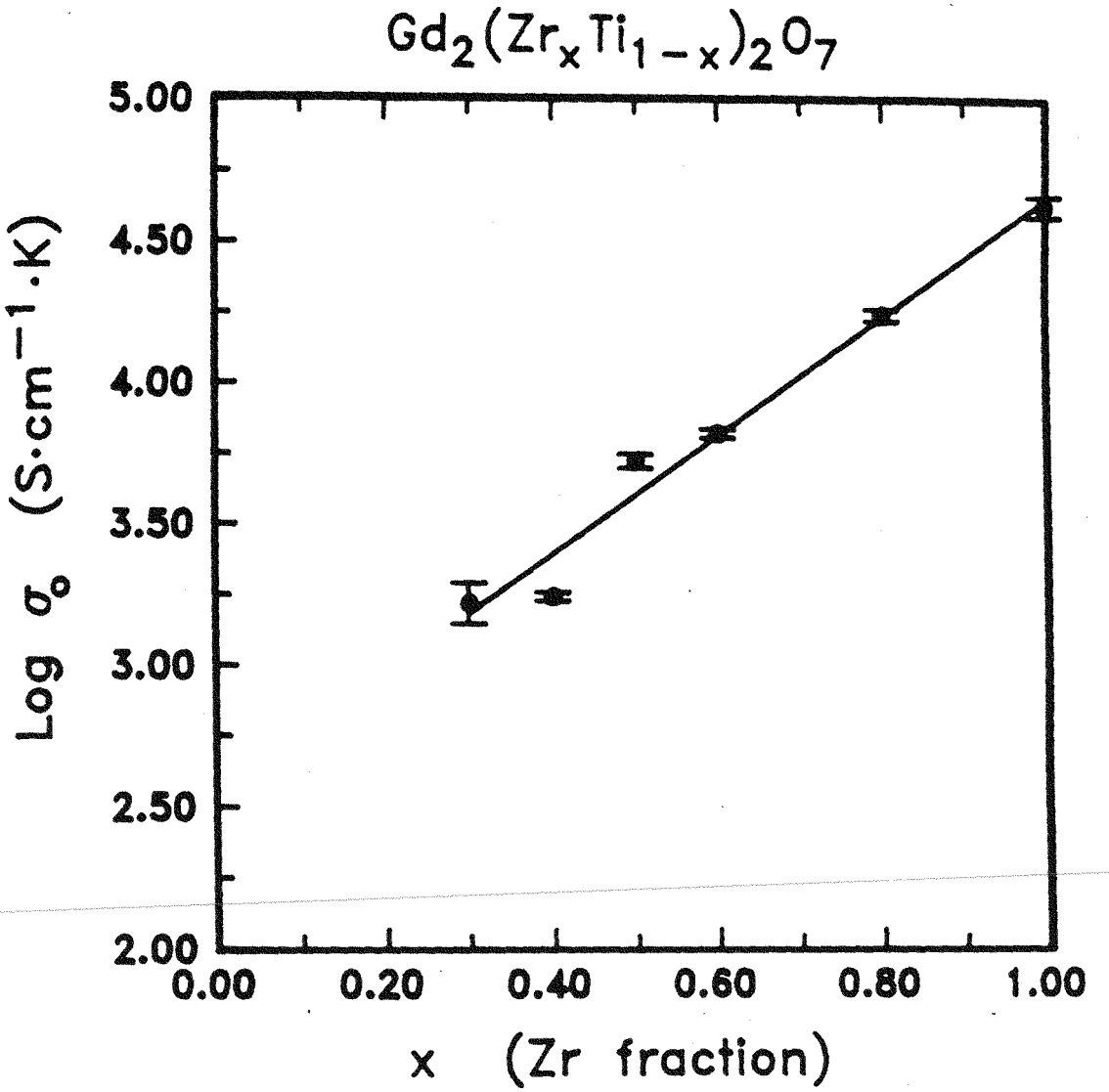

Fig. 10: The pre-exponential constant for ionic conduction as a function of composition for $Gd_2(Zr_xTi_{1-x})_2O_7$.

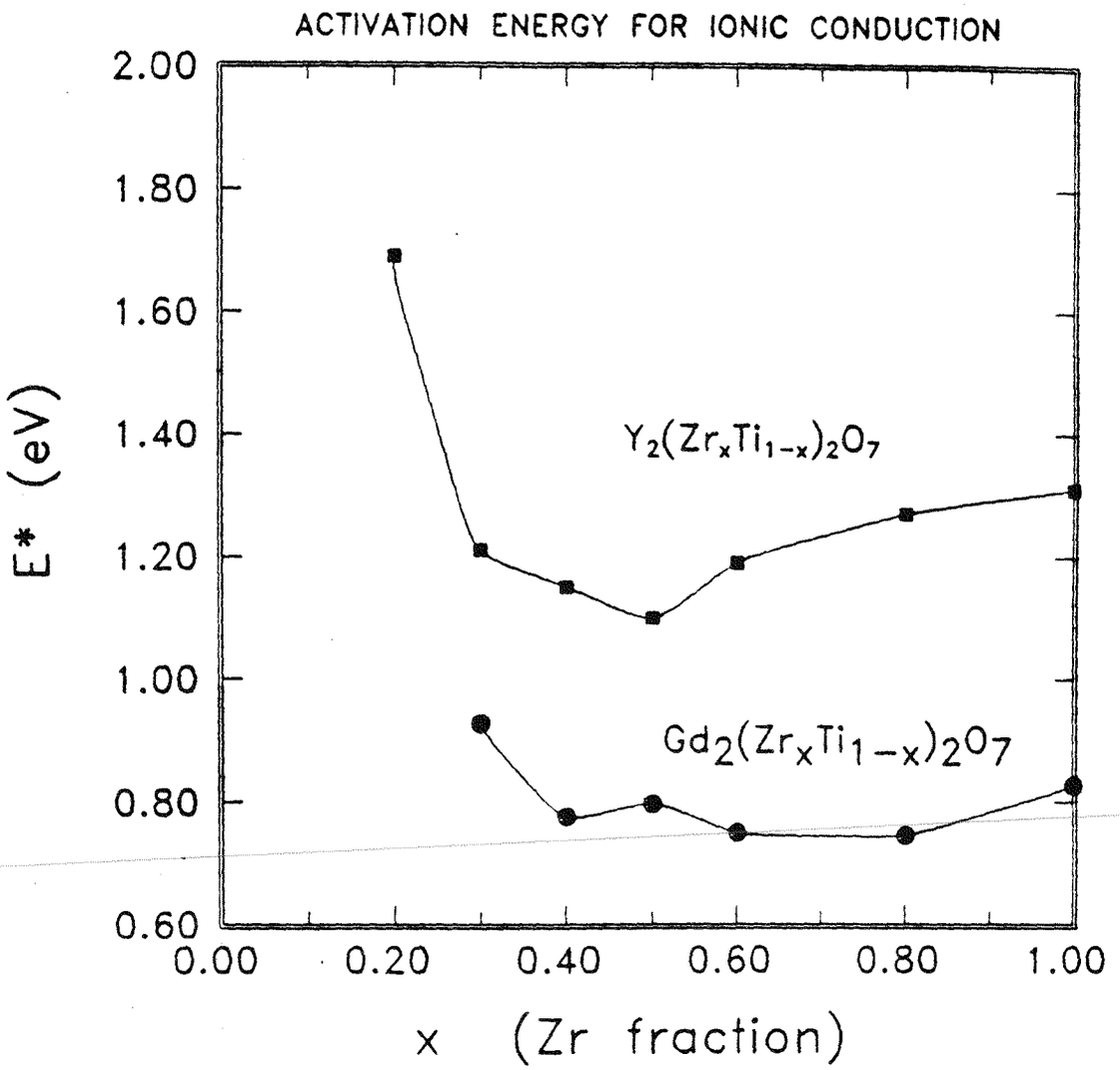

Fig. 11: Activation energy for ionic conduction in GZT and YZT as a function of Zr fraction.

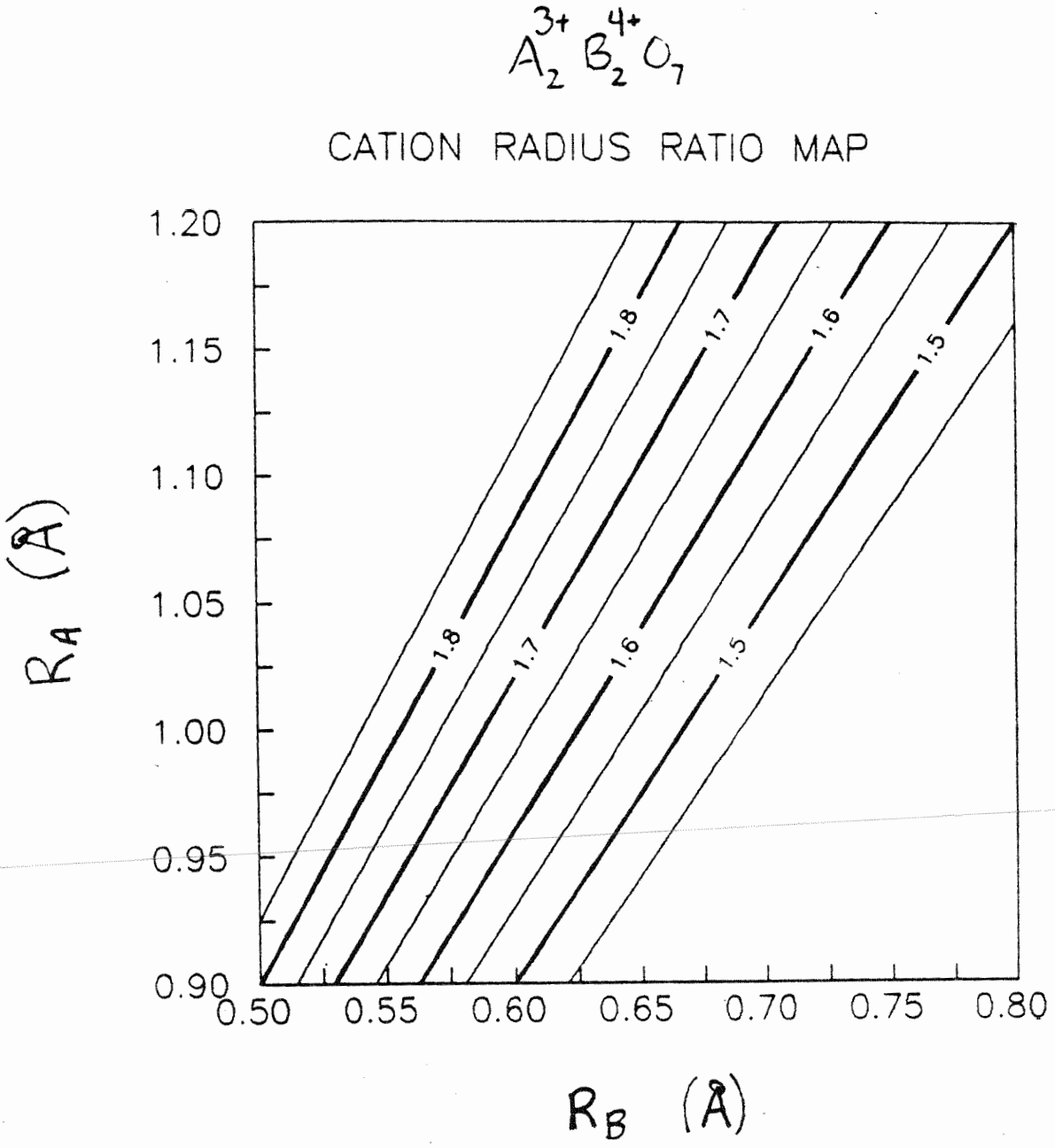

Fig. 12: Cation radius ratio map for pyrochlore compounds.

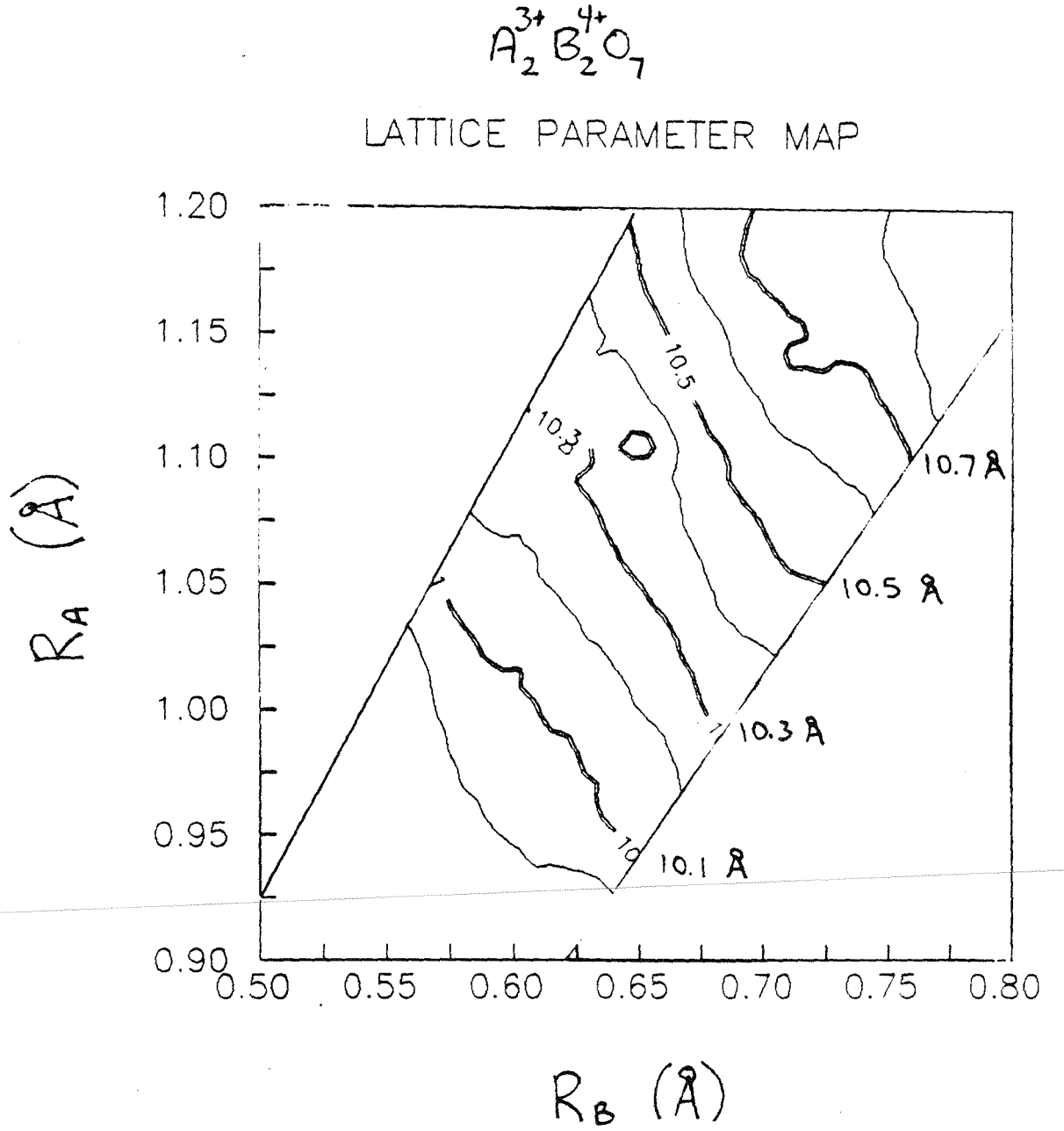

Fig. 13: Lattice parameter map for pyrochlore compounds. Curves labeled 10.1-10.7Å correspond to curves of constant lattice parameter.

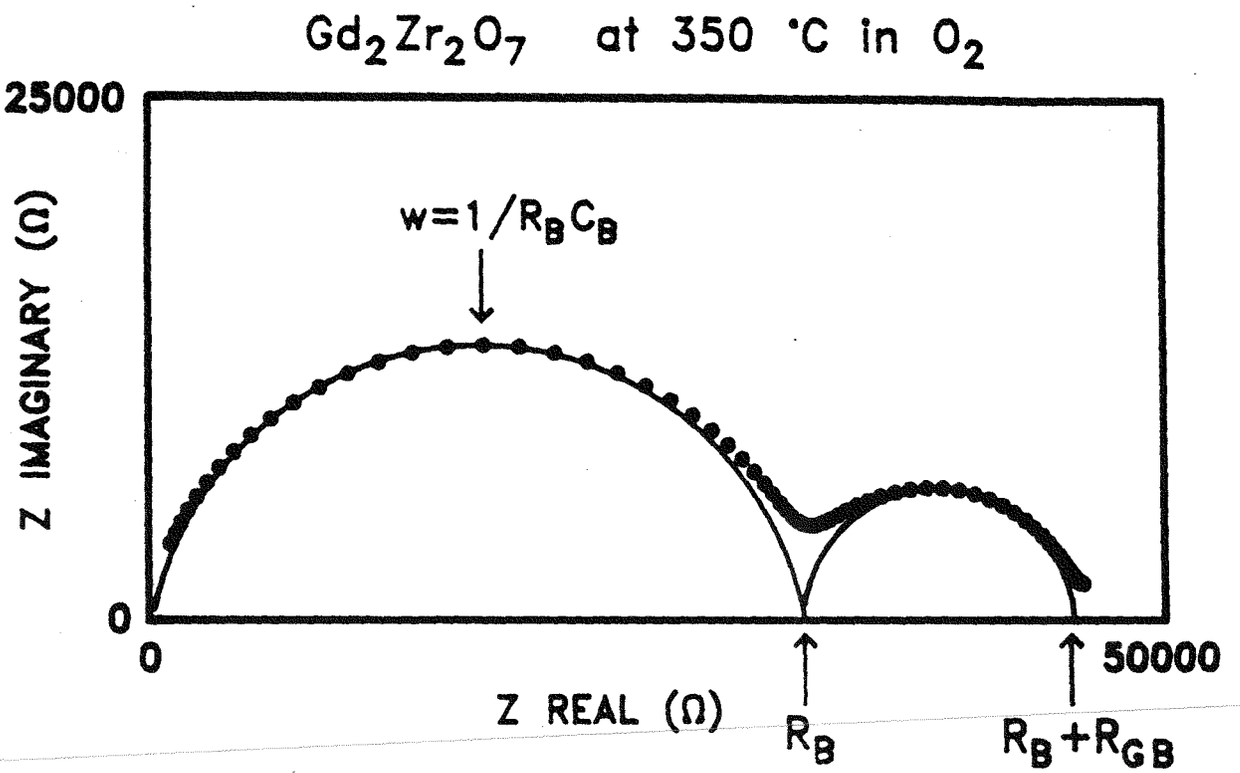

Fig. 14: A complex impedance plot for $Gd_2Zr_2O_7$ at 350°C in oxygen showing the assignment of bulk and grain boundary resistances.

APPENDIX A

Sample Preparation

We have chosen a sample preparation method that can produce high density, high purity ceramics with precisely known cation ratio. In this way, we avoid the sources of confusion that arise when porosity, impurities and molecularity are inadequately controlled. We are thus able to focus upon the effects of dopants and cation-anion stoichiometry in a well defined system.

Pyrochlore powder is synthesized by pyrolysis of metal-citrate complex precursors. This approach was developed for fabricating perovskites by Pechini[19] in 1967 and later modified slightly by Eror in 1970.[20]

The Pechini process uses metal-citrate complex formation followed by polyesterification and then organic removal by pyrolysis to generate homogeneous, uniform, sinterable powder with precisely controlled composition. The powder produced by the Pechini process is die pressed, isopressed, and sintered at ~1600°C to form relatively dense polycrystalline ceramic specimens.

We have generated ceramic specimens with compositions throughout the GZT and YZT solid solutions. We have also successfully produced both calcium and tantalum doped samples.

Electrical Conductivity Data

A variety of electrical impedance measurement instruments and an automated data acquisition system allow us to collect electrical conductivity data accurately and efficiently. At

present, our instrumentation includes an HP4192A impedance analyzer, Solartron 1250 frequency analyzer, HP4140B picoammeter/programmable voltage source, and IBM PC XT's and AT's for analysis and control.

The key electrical quantity to measure is the real, bulk conductivity. This is the quantity required for defect chemical model building. Since the bulk conductivity is generally masked by grain boundary and electrode effects, it is necessary to separate out these spurious effects. We have had good success separating out the bulk conductivity by an examination of the frequency dependence of the electrical impedance in complex impedance plots.

Figure 14 shows a complex impedance plot obtained from a sample of $Gd_2Zr_2O_7$ in the frequency domain. Once can see semicircles corresponding to the bulk and the grain boundary. The high frequency semicircle can be unambiguously assigned to the bulk on the basis of its apparent dielectric constant (ε = 60). This ability to clearly identify the magnitude of the bulk conductivity is a major feature of our work and occurs as a result of careful choice of the experimental system combined with state of the art equipment.

Structural Characterization

Powder x-ray diffraction measurements were made on a large number of samples in the $Gd_2(Zr_xTi_{1-x})_2O_7$ system. We were able to index every peak in every diffraction pattern using the

pyrochlore structure. This indicates that $Gd_2(Zr_xTi_{1-x})_2O_7$ is a true solid solution with a single phase for all values of x between 0 and 1.

The x-ray diffraction patterns were also used to obtain the lattice parameters as a function of composition. The results are shown in Figure 2. Within the limits of experimental error, the lattice parameter vs. composition curve is a straight line in accordance with Vegard's law. This is a further confirmation that $Gd_2(Zr_xTi_{1-x})_2O_7$ represents a single phase.

The x-ray diffraction patterns were also used to make careful, quantitative measurements of the area of selected diffraction peaks. A computer model was used to calculate the expected theoretical peak areas as a function of the cation order parameter. The cation order parameter is defined as 0 for complete disorder between the A and B cations in pyrochlore, i.e., $(AB)_2(AB)_2O_7$, and defined as 1 for complete order, i.e., $(A)_2(B)_2O_7$. By comparison of the computer model and the experimental data, we were able to estimate the cation order parameter as a function of composition. The results, as shown in Figure 6, are consistent with our expectations of increasing disorder with increasing Zr content as described above.

APPENDIX B

Neutron Powder-Diffraction Profile Analysis of Pyrochlore Solid Solutions* Perfomed in Collaboration with and Under the Supervision of Professor B.J. Wuensch, MIT

The conductivity of GZT and YZT as described above displays a marked change in magnitude as a function of the Zr content of the solid solution. As is the case with many fast ion conductors, the increase in conductivity is attributed to a structural change in the material. Specifically, in the present systems, the enhanced conductivity has been interpreted as arising from a decrease in anion order with increasing Zr content.

A detailed structural analysis based on neutron scattering data is to be perfomed for a series of phases which span the solid solution series in the $Y_2(Zr_xTi_{1-x})_2O_7$ system. The structural analysis will provide detailed insight into the nature and extent of the disorder, and precise values for the atomic coordinates, thus permitting quantitative determination, as a function of composition, of the saddle-point configuration at "windows" separating equilibrium positions of the ions along likely diffusion paths. Moreover, the analyses provide values for the parameters which describe the thermal motion of the atoms. Any anisotropy or anharmonicity observed in the thermal behavior of a mobile ion, or an increase in the vibrational amplitudes indicative of "softening" of a potential well with

*Note: Supplementary funding to initiate this work on YZT was provided in this year's (1988-89) budget. Extension of this work to other pyrochlores of interest is expected to continue during the three year renewal period.

change in composition provides important insight into the atomic-scale nature of the diffusion paths. In favorable cases, it is possible to extract the single-particle potential for the mobile ion and deduce an activation enthalpy for the diffusion process. Comparision of the value with that deduced from direct measurement of the conductivity provides a unique confirmation of the interpretation of the mechanism.

Neutron powder diffraction data will be collected and analyzed via Rietveld analysis to obtain the atomic coordinates, thermal vibration parameters, cation order parameter, and oxygen interstitial concentration as a function of compositon in the system $Y_2(Zr_xTi_{1-x})_2O_7$.

Initially, three compositions will be examined (x = 0, 0.3, and 0.6) which span the range of partial disorder. The powder samples necessary for the analysis will be subjected to annealing at 1350°C for a period of time necessary to achieve the equilibrium state of order characteristic of that temperature. Depending on the precision of the results obtained, further analyses may be performed for additional specimens at other intermediate compositions for which conductivity data have been obtained.

Diffraction data provide a precise description of the distribution of scattering density within an average unit cell in a crystalline material. The average represents both a time average of dynamic disorder (i.e., thermal vibration) as well as a positional average of static disorder within various cells in the material. It is possible to separate these influences

through determination of the structural parameters as a function of temperature as the anisotropic temperature-factor coefficients should increase in proportion to T and, moreover, should extrapolate to zero as temperature approaches zero. Both types of disorder occur in fast-ion conductors and the possibility of distinguishing between them provides further valuable insight into the atomic-scale nature of the conduction mechanism. Accordingly, depending on the results of the initial room-temperature analyses, it may be of interest to perform analyses as a function of temperature for one intermediate composition.

PUBLICATIONS RESULTING FROM THIS PROGRAM

The current funding program is now two years old. In this time, we have completed three papers and have a number more in preparation:

1. P.K. Moon and H.L. Tuller, "Fast Ion Conduction in $Gd_2(Zr_xTi_{1-x})_2O_7$," to be published in Proceedings of the NATO Advanced Study Institute for Fast Ion Conductors, July 1-15, 1987, in Erice, Italy, eds. H.L. Tuller and M. Balkanski (Plenum Press, New York).

2. P.K. Moon and H.L. Tuller, "Ionic Conduction in the $Gd_2(Zr_xTi_{1-x})_2O_7$ System," to be published in Proceedings of the Sixth International Conference on Solid State Ionics," Garmisch-Partenkirchen, FRG, September 6, 1987.

3. H.L. Tuller and P.K. Moon "Fast Ion Conductors-Future Trends," to be published in Materials Science & Engineering B (invited paper), in press.

4. P.K. Moon, M.A. Spears, and H.L. Tuller, "The Defect Chemistry of Pyrochlore Solid Solutions of the Type $R_2(Ti_{1-x}Zr_x)_2O_7$ with R = Gd,Y", Materials Research Society, December 1988, Boston, MA, in preparation.

5. P.K. Moon and H.L. Tuller, "Intrinsic Fast Oxygen Ionic Conductivity in the $Gd_2(Zr_xTi_{1-x})_2O_7$ Pyrochlore System," Materials Research Society, December 1988, Boston, MA, in preparation (invited paper).

6. M. Oueslati, M. Balkanski, P.K. Moon, and H.L. Tuller, "Raman Spectroscopy and Structural Disorder in $Gd_2(Zr_xTi_{1-x})_2O_7$," Materials Research Society, December 1988, Boston, MA, in preparation.